THE CLOSED STATE OF THIN FILAMENTS IN SKELETAL MUSCLE IS NOT RELEVANT DURING CONTRACTION UNDER PHYSIOLOGICAL CONDITIONS

Sergey Y. Bershitsky[1], Natalia A. Koubassova[2], Michael A. Ferenczi[3], Galina V. Kopylova[1],·Theyencheri Narayanan[4], Andrey K. Tsaturyan[2]

[1]Institute of Immunology and Physiology, Ural Branch of the Russian Academy of Sciences, Yekaterinburg, Russia
[2]Institute of Mechanics, M.V. Lomonosov Moscow University, 1 Michurinsky prosp., Moscow 119192, Russia
[3]Lee Kong Chian School of Medicine, Nanyang Technological University, Singapore 636921, Singapore
[4]European Synchrotron Radiation Facility, Grenoble, France

Key words: muscle contraction, regulation, tropomyosin, x-ray diffraction, modeling

Running title:

Corresponding author: tropomyosin movement in contracting muscle

Andrey Tsaturyan
Institute of Mechanics
Moscow University
1 Mitchurinsky prosp.
Moscow 119192 Russia

E-mail: tsat@imec.msu.ru

ABSTRACT

Muscle contraction is powered by actin-myosin interaction controlled by Ca^{2+} via regulatory proteins, troponin (Tn) and tropomyosin (Tpm), associated with actin filaments. Tpm forms coiled-coil dimers, which assemble into a continuous helical strand that runs along the whole ~1 μm length of a thin filament. In the absence of Ca^{2+}, Tn that is tightly bound to Tpm binds actin and holds Tpm strand in the blocked, or B, state where Tpm shields actin from the binding of myosin heads. Ca^{2+} binding to Tn releases Tpm from actin, so that it rotates around filament axis to a closed, or C, state where actin is partially available for weak binding of myosin heads. Upon transition of the weak actin-myosin bond into strong, stereo-specific complex, the head pushes Tpm strand to the open, or O, state allowing myosin binding sites on several neighbor actin monomers to become open for myosin binding. We used low-angle x-ray diffraction at the European Synchrotron Radiation Facility to check whether the O- to C-state transition of fully activated fibers of fast skeletal muscle of the rabbit occurs at near physiological conditions, *i.e.* during transition from isometric contraction to shortening under low load. No decrease in the intensity of the second actin layer line A2 at reciprocal radii in the range of 0.15-0.275 nm^{-1} was observed during shortening suggesting that an azimuthal Tpm movement from the O- to C-state does not occur, although a reduction in the muscle stiffness and the intensities of other actin layer lines demonstrated that a ~2-fold decrease in the fraction of myosin heads strongly bound to actin accompanies shortening. The data show that a small fraction of actin-bound myosin heads is sufficient for supporting the O-state and, therefore the C-state is probably not relevant for fully activated skeletal muscle that produces mechanical work at low load.

INTRODUCTION

Muscle contraction is powered by an interaction of myosin heads with actin monomers, which form the backbone of thin filaments. The fuel for work production by the actin-myosin motor is ATP hydrolysis. Contraction and relaxation of skeletal and cardiac muscles are regulated by Ca^{2+} ions *via* regulatory proteins, troponin (Tn) and tropomyosin (Tpm), associated with the actin filaments to form Ca^{2+}-regulated thin filaments. Tpm is a coiled-coil dimer that lies on the surface of the actin filament in a long helical groove with a pitch of *ca*. 36 nm. Tpm dimers bind each other in a head-to-tail manner to form two continuous strands running along the whole length of an actin filament. Tn consists of three subunits: Tn-C, Tn-I and Tn-T. The steric blocking model proposed more than 40 years ago (Haselgrove, 1972; Vibert et al., 1972; Huxley, 1972; Spudich et al., 1972) suggests that in the absence of Ca^{2+}, Tpm closes myosin-binding sites on actin and thus keeps muscle in the relaxed state. Ca^{2+} binding to Tn-C releases Tn-I from actin and allows Tpm to move azimuthally around the thin filament axis and enables myosin binding to actin. Later MacKillop and Geeves (1993) suggested a more detailed three-state model based on biochemical studies. Their model was later supported by electron microscopy (EM, Vibert et al., 1997). According to this model that was later combined with a crystallography-based model of Ca^{2+}-regulation of Tn (Vinogradova et al., 2005), in the absence of Ca^{2+}, a mobile inhibitory segment of Tn-I binds actin and keeps the Tn-Tpm strand in a position where it covers the myosin binding sites on actin (blocked, or B-state) thus making them inaccessible to myosin. In the B-state muscle is relaxed. Ca^{2+} binding to Tn-C opens a hydrophobic pocket between the long □-helix and the Ca^{2+}-binding domain of Tn-C. The switch segment of Tn-I located in the vicinity of the inhibitory segment binds the pocket, releases the Tn-Tpm complex from actin and causes Tpm rotation around the filament axis by ~25□. In this closed, or C-state, myosin heads attach to actin monomers on the filament to form weakly bound complexes. Subsequent transition of the actin-myosin complex to a strongly, stereo-specifically bound form causes further Tpm rotation by ~10□ to the open, or O-state, of the regulatory system.

As both biochemical and EM data were obtained *in vitro*, where the transition between the C- and O-states was induced by a saturating concentration of myosin heads, the question remains whether the transition takes place in fully activated contracting muscle upon a change in the fraction of myosin heads bound to actin in physiological conditions. To monitor changes in the Tpm azimuthal position we used low angle x-ray diffraction. This approach was used 40 years ago for monitoring the B- to C-state transition during the onset of contraction of skeletal frog muscle by Kress et al. (1986) who measured the time course of the changes in the intensity of the second actin layer line, A2, with a meridional spacing of ~$(18\ nm)^{]1}$ at a radial spacing of

~(24 nm)$^{-1}$. They found that the B- to C-state transition precedes not only tension rise but also changes in the equatorial x-ray reflections, which reflect the mass transfer from thick (myosin) to thin (actin) filaments. Although it is likely that in the experiments of Kress et al. (1986) ~~most probably~~ two subsequent transitions took place, firstly from the B- to C- and then from C- to the O-state ~~took place~~, the authors were not able to distinguish between them and observed a monotonic transient.

Here we report the results of measurement of changes in the 2D diffraction patterns ~~from~~in fully activated rabbit muscle fibres. The membrane of the fibres were ~~with~~ permeabilized to allow complete control of the myofibrillar space. ~~membrane,~~ The change in activated state was caused by a transition from isometric contraction to steady shortening under a load in the range of 28-38% of the isometric level, at a constant temperature in the range~~of~~ 26-32°. Such a transition is accompanied by a substantial reduction in muscle stiffness (Julian, Morgan, 1981; Ford et al., 1985) suggesting that the fraction of the myosin heads strongly bound to actin also decreases substantially during shortening. Tpm movement was monitored by measuring the intensity of the A2 actin layer a reciprocal radii range of 0.15-0.275 nm^{-1} in the low angle x-ray diffraction pattern. Simulation performed using high resolution models of the actin-Tpm complexes shows that in this radial range the A2 intensity depends on the azimuthal Tpm movement independently on the fraction of myosin heads bound to actin (Koubassova, 2016). No evidence of a C- to O- transition was detected during the change in state from isometric to shortening.

MATERIAL AND METHODS

Muscle fiber samples and apparatus

Experiments were performed with thin bundles of three fibers from *m. psoas* of the rabbit, which were dissected, prepared and stored as described previously (Ferenczi *et al*., 2005). The instruments and processes were described previously, including the Joule temperature-jump (T-jump) set-up, the change and measurement of muscle length and force, the remote control system and the composition of experimental solutions (Tsaturyan et al., 2011).

X-ray diffraction experiments

The experiments were carried out at beam line ID02 (ESRF, Grenoble, France) at constant wavelength of ~0.1 nm at x-ray flux of 3.7-3.8 × 10^{13} photons/s. The x-ray beam was focused on the FReLoN CCD detector. Two series of experiments with identical protocol, but different detector-to-sample distances and detector resolution were performed. In the first series of 6 experiments, the detector operating at 1024 × 256 pixel resolution was placed 2.25 m from the

sample; the beam size at the vertically-mounted fiber was 200 × 300 μm (vertically × horizontally, FWHM). In the second set of 6 experiments a broader range of reciprocal spaces up to 0.31 nm^{-1} was examined: the detector operated at 480 × 480 pixel resolution and was placed 1.5 m from the sample; the beam size on the sample was 200 × 400 μm (vertically × horizontally, FWHM).

Experimental protocol

A bundle of 3 muscle fibers was activated by transfer from the relaxing to the activating solution containing 30 μM Ca^{2+} at 0-2°C at sarcomere length of 2.4-2.45 μm. After several seconds the bundle was transferred to an empty trough where its temperature increased to 4-5°C. The bundle was then subjected to a T-jump of 22-27°C amplitude that increased its temperature to 26-32°C. When steady-state isometric tension has developed, the bundle was exposed to the x-rays for 10-15 ms and the diffraction pattern was recorded at the detector. Then, a small length step shortening was applied to the bundle followed by a ramp shortening at a velocity of 1.2-1.5 muscle length per second so that tension decreased and reached a near steady-state level of 0.28-0.38 of the isometric value. At the end of shortening ~~of the~~with a total amplitude of 4-5.5% of the initial bundle length, another x-ray diffraction pattern was recorded. The exposure time for the two frames were equal. In some experiments small step stretches of ~0.3% of fiber length accomplished in 0.15 ms were applied just after each x-ray frame to measure instantaneous muscle stiffness (Fig. 1). The mechanical responses to a T-jump, step stretches and shortening in a representative experiment, and the signal of the electrically-operated x-ray shutter opening ~~taken from~~detected by a pin diode are shown in Fig. 1. The protocol was repeated several times in each of 6 fiber bundles, in each of two series of experiments until isometric tension at the higher temperature decreased to 85% of its initial level or the bundle broke. Isometric force at 26-32°C was 217±17 kN/m^2 (mean±S.E.M., n=12, full range 150-305 kN/m^2).

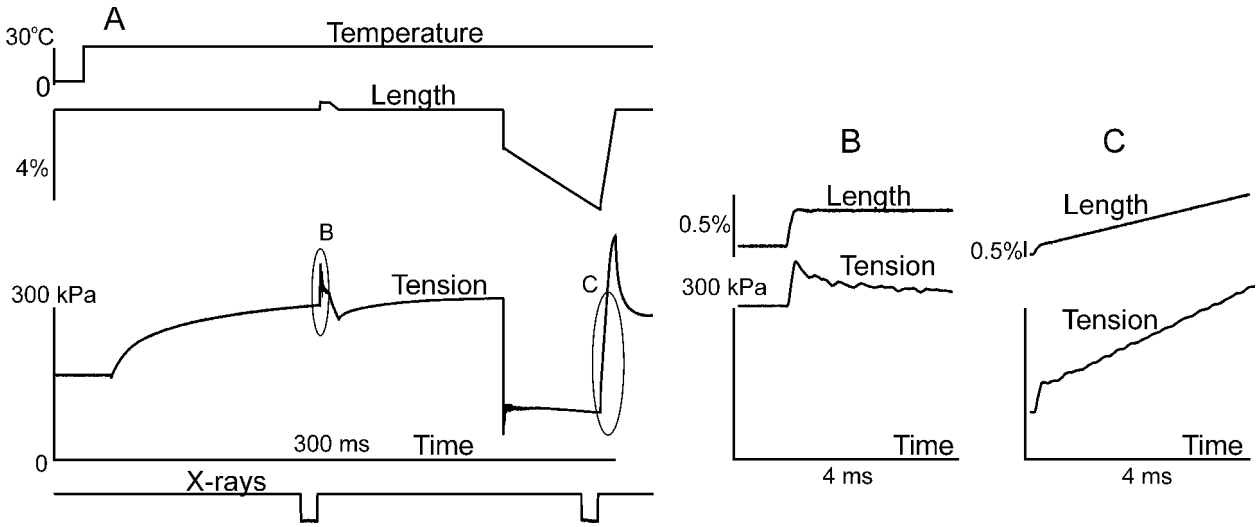

Fig. 1. A typical time course of temperature, length change, tension and x-ray shutter opening signal during a run of the experimental protocol in a bundle of 3 muscle fibers (from top to bottom, *A*). Step stretches were applied to the bundle immediately after each x-ray frame to measure instantaneous stiffness. These parts of the record are shown by ellipses *B* and *C* in *A* and on an expanded time scale in *B* and *C*, respectively.

Data analysis and modeling

To correct for an increase in the bundle volume exposed to the x-rays during shortening, the second pattern was divided by a factor of the average shortening of the bundle in the middle of the 2nd frame (Fig. 1). The factor was 1.04–1.06 depending on the amount of shortening at the middle of the second x-ray exposure. The diffraction patterns collected in all runs of an identical protocol before and during shortening were added together. The background x-ray signal was subtracted and the patterns were mirrored as described previously (Tsaturyan et al., 2011). The meridional and off-meridional x-ray intensities were obtained using radial integration and background subtraction as described by Tsaturyan et al. (2011). The regions of radial integration were as follows: 0-0.02 nm^{-1} (meridian), 0.02-0.036 nm^{-1} (1,0 row line), 0.036-0.063 nm^{-1} (1,1 row line), 0.063-0.15 nm^{-1}, and 0.15-0.275 nm^{-1} (high angle). It was shown that the peak of the 1st myosin layer line, M1, is located within the 1,0 row line, while that of 1st actin layer line, A1, is located within the 1,1 row line (Bordas et al., 1993; Tsaturyan et al., 2011). Modeling based on recent high resolution structural models of the actin-Tpm-myosin complex shows that the contribution of actin-bound myosin heads to actin layer lines A1 and A2 is limited to the range of reciprocal radii <0.15 nm^{-1} (Koubassova 2016).

RESULTS

Changes in instantaneous muscle stiffness upon transition from isometric contraction to shortening

To measure changes in instantaneous muscle stiffness caused by transition from isometric contraction to steady shortening under low load step, rapid stretches by ~0.3% of muscle length completed in 0.16 ms were applied to the bundles just after the end of the 1st and 2nd x-ray exposure during the protocol (Fig. 1). Upon shortening stiffness decreased from 32.6 MPa to 17.9 MPa (Fig. 1), *i.e.* to 55% of its isometric value. On average, the shortening load was ~~The ratio of muscle stiffness during shortening under load of~~ 28-38% of isometric. The average stiffness during shortening was ~~to that on plateau of isometric contraction was~~ 63□6% (mean□S.D., *n*=5) of that in isometric conditions.

Changes in the x-ray actin layer lines caused by muscle shortening

The intensities of the off-meridional x-ray reflections integrated at the reciprocal radii of 0.02-0.15 nm^{-1} during isometric contraction and at the end of steady shortening collected in a set of experiments with longer camera length and higher detector resolution are shown in Fig. 2.

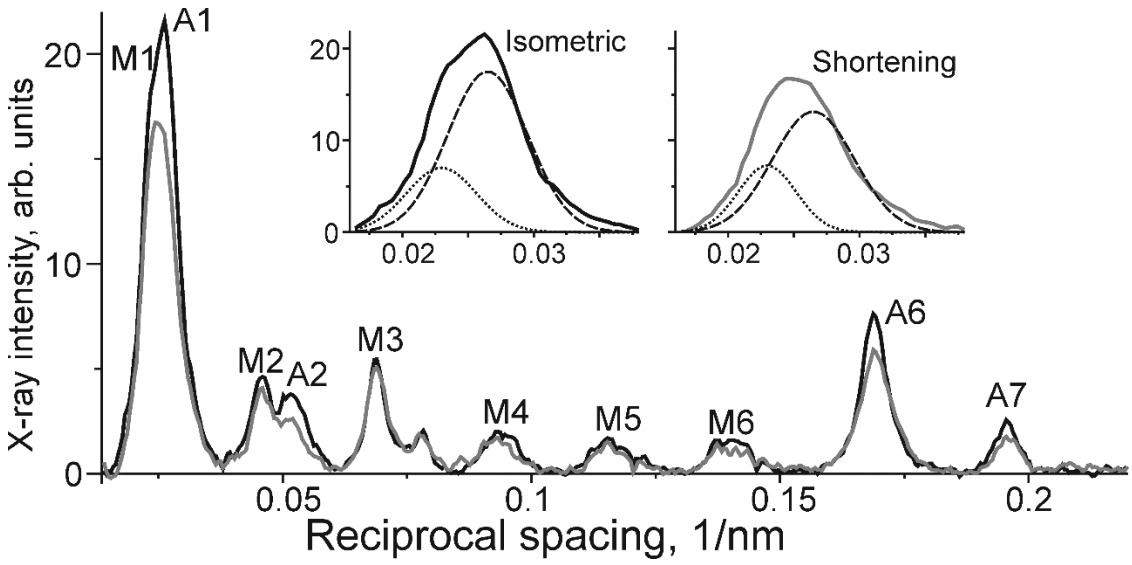

Fig. 2. Off-meridional x-ray intensity, collected from 43 runs of the experimental protocol in 6 bundles of muscle fibers during isometric contraction (black lines) and steady shortening (gray lines), integrated at reciprocal radii from 0.005 to 0.15 nm^{-1}. Some myosin (M) and actin (A) layer lines are labelled. Inset: intensity profiles in the region of M1 and A1 layer lines, and their breakdown into their Gaussian components, namely the M1 (dotted lines) and A1 (dashed lines) during isometric contraction and shortening.

The transition from isometric contraction to steady shortening under low load caused a decrease in the intensity of the actin but not of the myosin layer line (Fig. 1). As the most informative (Koubassova et al., 2008; Tsaturyan et al., 2011) first actin layer line, A1, was not separated from the neighbor myosin M1 layer line, we estimated the amount of the decrease in the A1 intensity, I_{A1}, using method 2 described by Tsaturyan et al. (2011)~~,~~ Nnamely, we fitted the profile of the combined M1/A1 actin layer to two Gaussian profiles which correspond to the M1 and A1 components. The results of such analysis are shown in the insets in Fig. 2. Upon shortening, the A1 component decreased to 75% of its isometric level while the M1 component did not change intensity. The A6 and A7 intensities, I_{A6} and I_{A7}, also decreased to 82% and 71% of their isometric levels, respectively, when isometrically contracting muscle bundles were allowed to shorten under a load of about a third of isometric tension (Figs. 2, 3).

Changes in the high angle part of the actin layer lines caused by shortening

X-ray intensities obtained in another set of experiments with a shorter camera allowed us to estimate changes in the actin layer lines A1 and A2 in the radial range up to 0.3 nm^{-1}. The results of those experiments are presented in Fig. 3.

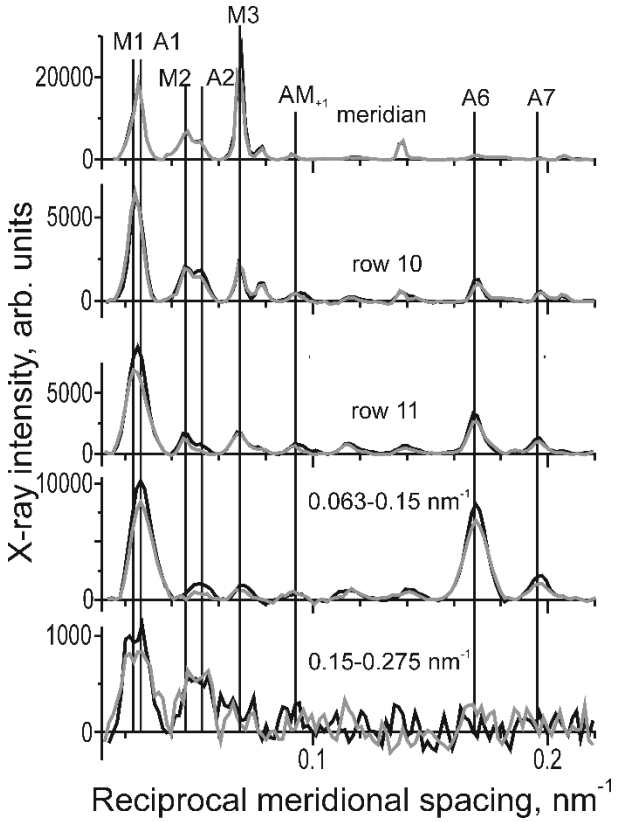

Fig. 3. Meridional profiles of x-ray intensity profiles calculated at different reciprocal radii during isometric contraction (black lines) and at the end of shortening (gray lines). The positions of the actin (A1, A2, A6, A7), myosin (M1, M2, M3) and actin-myosin (AM_{+1}) layer lines are labeled.

The only pronounced change in the meridian is a decrease in the intensity of the myosin meridional reflection M3 upon transition from isometric contraction to a steady shortening. ~~For the first time such~~This shortening-induced decrease in the M3 intensity ~~in whole frog muscle~~ was discovered by Huxley et al. (1983) in whole frog muscle. The off-meridional intensities of the actin layer lines A1, A2, A6, and A7 and the beating actin-myosin layer line AM_{+1} at ~(10.3 nm)$^{-1}$ at reciprocal radii up to 0.15 nm^{-1} decreased upon shortening. As myosin heads strongly bound to actin contribute to the intensities of the actin layer lines in this range of reciprocal radii (Koubassova et al., 2008; Koubassova et al., 2016), the data suggest that during shortening the fraction of such myosin heads becomes lower than that during isometric contraction.

In contrast, at reciprocal radii more than 0.15 nm^{-1} the intensity of the A2 layer line did not change upon the transition from isometric state to the shortening. The amplitude of the peak on the outer part of the A1 layer line decreased slightly while its width somewhat increased (Fig. 3), so that the total A1 intensity did not change significantly.

Modeling of the x-ray diffraction pattern

To find the regions in the x-ray diffraction pattern where changes in the intensity unambiguously report the Tpm movement independently from the fraction of myosin heads bound to actin, we performed direct modeling of the diffraction patterns at different positions of the tropomyosin strand on thin filaments and different fractions of myosin heads bound to actin. For this, the structural model of Behrmann et al. (2012) and a direct modeling approach (Koubassova et al., 2008; 2016) were used. Calculations were performed for the fractions of 0%, 20% and 40% of myosin heads stereo-specifically bound to actin. The results of these calculations are shown in Fig. 4.

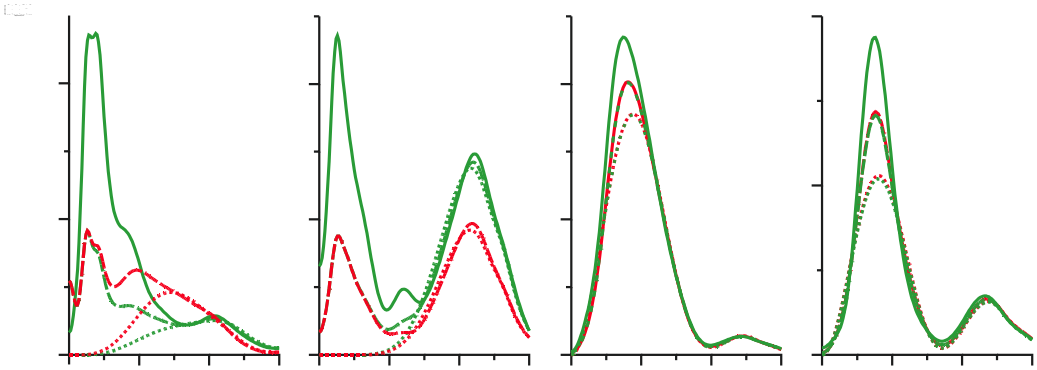

Fig. 4. The intensities of A1, A2, A6, and A7 actin layer lines calculated at different positions of the tropomyosin strand on the thin filament and with different fractions of myosin heads bound to actin. What azimuthal range? Continuous, dashed and dotted lines correspond to 40%, 20%, and 0% of myosin heads strongly bound to actin; green and red lines correspond to the ‘open’ (O-state) and ‘closed’ (C-state) positions of Tpm, respectively. The O-state is the original structural model (Behrmann et al., 2012) while the C-state was obtained by rotation of the Tmp strand around the thin filament axis by 10□. The figure axes need to be labelled and marked A1, A2, A6, A7

As expected, the contribution of the actin-bound myosin heads to the A1 and A2 actin layer lines is limited to the range of 0–0.15 nm^{-1}. Outside this range, the A1 and A2 intensities depend only on the position of the Tpm strand on the thin filament and can be used for

monitoring the transitions between different states of the regulatory proteins. On the other hand, the intensities of the A6 and A7 actin layer lines do not depend on the Tmp position.

DISCUSSION

X-ray diffraction measurement of Tpm movement

A number of models have been suggested to interpret the observed changes in the intensities of the actin layer lines in terms of Tpm movement on the surface of the actin filament (Al-Khayat et al., 1995; Poole et al., 2006; Koubassova, 2008). As these models are based on low resolution structures, ~~none of them~~they do not provide a quantitative description of the x-ray intensities observed in muscle diffraction experiments. Even the ratio of the intensities of bright A6 and A7 actin layer lines with spacings of ~(5.9 nm)$^{-1}$ and ~(5.1 nm)$^{-1}$ were not reproduced correctly in models for a spatial resolution worse than 2-2.5 nm (Koubassova, 2008). In contrast to those early models, models based on new high resolution EM structures (Behrmann et al., 2012; von der Ecken et al., 2015) provide a quantitative fit to the A2, A6, and A7 actin layer lines (Koubassova et al., 2016). The results of the modeling suggest that the A2 intensity at reciprocal radial range of 0.15-0.3 nm^{-1} gives a reliable index of Tpm rotation, unaffected by contamination of other reflections. Most pertinently, as shown in Fig. 4, this intensity is not affected by the presence of the actin-bound myosin heads. Calculations show that the transition from the O- to C-state should result in 35-58% reduction of the A2 intensity at reciprocal radii of 0.15-0.275 nm^{-1} (Koubassova et al., 2016). The most conservative estimate assuming 10□ Tpm rotation predicts a 35-40% decrease in the high angle part of A2 intensity (Fig. 4).

Reduction in the fraction of actin bound myosin heads upon shortening

Our stiffness measurements (Fig. 1) show~~ed~~ that during shortening instantaneous muscle stiffness decreased to ~63% of its isometric level. A substantial fraction of compliance of contracting muscle is caused by compliance of the actin and myosin filaments (Huxley et al., 1994). For permeabilized fibers from rabbit muscle, the filament compliance was estimated to be 19 nm/MPa per half sarcomere, i.e. about ~~a~~ half of the compliance of isometrically contracting muscle is caused by filaments compliance (Caremani, ,2008). Taking into account that filament compliance is connected in series with that of the crossbridge~~s one~~, the increase in the compliance by a factor of 1/0.63 = 1.58 upon muscle shortening corresponds to an increase in the crossbridge compliance by at least a factor of two: 1.58 } 0.5 = 1.08 *vs.* 1. } 0.5 =0.5. We therefore conclude that the fraction of actin-bound myosin heads which contribute to muscle stiffness was reduced by at least a factor of two after transition from isometric contraction to steady shortening under load of about a third of its isometric level.

A decrease in the A1, A2, A6 and A7 intensities also suggests that shortening induced a substantial decrease in the fraction of myosin heads stereo-specifically bound to actin. The decrease estimated from the decrease in I_{A1} using the approach developed previously (Tsaturyan et al., 2011) also suggests a ~2-fold decrease in this fraction. Changes in the intensities of the A6 and A7 layer lines upon a transition from isometric contraction to a steady shortening at a load of about a third of isometric tension found here (Figs. 2, 3) were similar to those observed in whole frog muscle (Yagi, Takemori, 1995; Yagi et al., 2006). Such changes are predicted by a model (Koubassova et al., 2016) in which the fraction of strongly bound myosin heads decreases from 40% to 20% (Fig. 4). As the fraction of strongly bound myosin heads during isometric contraction at a near-physiological temperature is ~40% (Tsaturyan et al., 2011), we estimate that during shortening in our experiments this fraction decreased to ~20% of all myosin heads being strongly bound during muscle shortening at a velocity of 1.2 – 1.5 muscle lengths/second at 26-32□C.

How many strongly bound myosin heads are needed to keep Tpm in the O-state

The absence of a decrease in the A2 intensity at reciprocal radii above 0.15 nm^{-1} suggests that a ~2-fold reduction in the fraction of the actin-bound myosin heads does not induce the O- to C-state transition in the Tpm position on thin filament. This means that even a small fraction of myosin heads strongly bound to actin during muscle shortening is sufficient for keeping Tpm in the O-state. Taking this fraction to be 20% of the total number of 300 myosin heads per a half of thick filament, we obtain 300□0.2 = 60 strongly bound heads. As the number of actin filaments is twice that of myosin filaments and there are two Tpm strands running along each thin filament, in average we have 15 myosin heads strongly bound to actin monomers in each actin filament region controlled by a Tpm strand. Taking the length of the overlap zone of thin and thick filaments to be ~750 nm at full filament overlap in the sarcomeres, one obtains the average distance between myosin heads strongly bound to actin along a Tpm strand to be 50 nm. The theory of Smith et al. (2003) and Smith, Geeves (2003) suggests that the persistence length of the Tpm strand that is considered as an elastic beam held in the vicinity of its position in the C-state by electrostatic forces between Tpm and the actin surface is ~20 nm. Thus, on average, a single myosin head strongly bound to actin is able to maintain the O-state of the Tpm segment over a distance of ~40 nm (2□20 nm). Later, a more precise theory was suggested (Metalnikova, Tsaturyan, 2013) that accounts for the intrinsic helical shape of the Tpm strand. It turned out that the helical shape of the beam produces effective tension in the Tpm strand making it similar to a stretched string. This tension increases the effective length of a Tpm segment that is involved in the azimuthal shift of the protein filament when a myosin head binds strongly to actin. Estimates made by Metalnikova, Tsaturyan (2013, Fig. S1) show that the ‘helicity induced tensile force’

increases the effective length of the Tpm strand involved into the C- to O-state transition induced by binding of a single myosin head by a factor of ~2. Therefore, the length of the Tmp segment involved into azimuthal movement upon binding of a head to actin is twice that estimated previously, and is about 80 nm. This explains why at the average distance between myosin heads strongly bound to actin along the Tpm strand of ~50 nm the strand remains in the O-state.

CONCLUSION

Our data suggest that at near physiological temperatures, the C-state is not relevant during contraction ~~and~~or shortening of fully activated skeletal muscle under physiological conditions: when Tn-C is fully saturated with Ca^{2+}, even the small fraction of myosin heads which remain bound to actin during muscle shortening is sufficient to maintain the regulatory system in the open state. Only the blocked and open states need to be considered for contraction and relaxation under physiological conditions. Can we say that Kress et al ‘s description was actually correct at the time, even though they lacked the resolution?

ACKNOWLEDGMENT

The beam time at beam line ID02 was provided by ESRF. Work was supported by grant No 16-14-10044 from the Russian Science Foundation (to SB).

REFERENCES

Vibert P.J., Haselgrove J.C., Lowy J., Poulsen F.R. 1972. Structural changes in actin-containing filaments of muscle. J. Mol. Biol. 71:757-67.

Spudich J.A., Huxley H.E., Finch J.T. 1972. Regulation of skeletal muscle contraction. II. Structural studies of the interaction of the tropomyosin-troponin complex with actin. J. Mol. Biol. 72:619-32.

Kress M., Huxley H.E., Faruqi A.R., Hendrix J. 1986. Structural changes during activation of frog muscle studied by time-resolved X-ray diffraction. J. Mol. Biol. 188:325-42.

McKillop D.F., Geeves M.A. 1993. Regulation of the interaction between actin and myosin subfragment 1: evidence for three states of the thin filament. Biophys. J. 65:693-701.

Vinogradova M.V., Stone D.B., Malanina G.G., Karatzaferi C., Cooke R., Mendelson R.A., Fletterick R.J. 2005. Ca(2+)-regulated structural changes in troponin. Proc. Natl. Acad. Sci. USA. 102:5038-43.

Ford L.E., Huxley A.F., Simmons R.M. 1986. Tension transients during steady shortening of frog muscle fibres. J. Physiol. 361:131-50.

Julian F.J., Morgan D.L. 1981. Variation of muscle stiffness with tension during tension transients and constant velocity shortening in the frog. J. Physiol. 319:193-203.

Tsaturyan A.K., Bershitsky S.Y., Koubassova N.A., Fernandez M., Narayanan T., Ferenczi M.A. 2011. The fraction of myosin motors that participate in isometric contraction of rabbit muscle fibers at near-physiological temperature. Biophys. J. 101:404-10.

Ferenczi M.A., Bershitsky S.Y., Tsaturyan A.K. 2005. The “roll and lock” mechanism of force generation in muscle. Structure. 13:131–141.

Behrmann E., Müller M., Penczek P.A., Mannherz H.G., Manstein D.J., Raunser S. 2012. Structure of the rigor actin-tropomyosin-myosin complex. Cell. 150:327-38.

Koubassova NA, Bershitsky SY, Ferenczi MA, Narayanan T, Tsaturyan AK. 2016. Tropomyosin movement is described by a quantitative high-resolution model of X-ray diffraction of contracting muscle. Eur. Biophys. J. 2016 Sep 17. [Epub ahead of print], PMID: 27640143.

Huxley H.E., Simmons R.M., Faruqi A.R., Kress M., Bordas J., Koch M.H. 1983. Changes in the X-ray reflections from contracting muscle during rapid mechanical transients and their structural implications. J Mol Biol. 169:469-506.

Yagi N., Takemori S. 1995. Structural changes in myosin cross-bridges during shortening of frog skeletal muscle. J. Muscle. Res. Cell. Motil. 16:57-63.

Yagi N., Iwamoto H., Inoue K. 2006. Structural changes of cross-bridges on transition from isometric to shortening state in frog skeletal muscle. Biophys J. 91:4110-20.

al-Khayat H.A., Yagi N., Squire J.M. 1995. Structural changes in actin-tropomyosin during muscle regulation: computer modelling of low-angle X-ray diffraction data. J. Mol. Biol. 252:611-32.

Poole K.J., Lorenz M., Evans G., Rosenbaum G., Pirani A., Craig R., Tobacman L.S., Lehman W., Holmes K.C. 2006. A comparison of muscle thin filament models obtained from electron microscopy reconstructions and low-angle X-ray fibre diagrams from non-overlap muscle. J Struct. Biol. 155:273-84.

Koubassova NA. 2008. A comparison of the models of a thin filament in the muscle with low-angle X-ray diffraction data obtained for the relaxed rabbit muscle. Biofizika. 53(6):936-42.

von der Ecken J., Müller M., Lehman W., Manstein D.J., Penczek P.A., Raunser S. 2015. Structure of the F-actin-tropomyosin complex. Nature. 519:114-7.

Smith D.A., Geeves M.A. 2003. Cooperative regulation of myosin-actin interactions by a continuous flexible chain II: actin-tropomyosin-troponin and regulation by calcium. Biophys. J. 84:3168-80.

Smith D.A., Maytum R., Geeves M.A. 2003. Cooperative regulation of myosin-actin interactions by a continuous flexible chain I: actin-tropomyosin systems. Biophys J. 84:3155-67.

Metalnikova NA, Tsaturyan AK.2013. A mechanistic model of Ca regulation of thin filaments in cardiac muscle. Biophys. J. 105:941-50.

Huxley H.E. 1972. Structural changes in the actin- and myosin-containing filaments during contraction; the mechanism of muscle contraction. Cold Spring Harbor Laboratory, Cold Spring Harbor, pp. 361–368.

Haselgrove J.C. 1972. X-ray evidence for a conformational change in the actin-containing filaments of vertebrate striated muscle. The Mechanism of Muscle Contraction. Cold Spring Harbor Laboratory; Cold Spring Harbor, pp 341–352.

Vibert P., Craig R., Lehman W. 1997. Steric-model for activation of muscle thin filaments. J. Mol. Biol. 266:8-14.

Koubassova N.A., Tsaturyan A.K. 2002 Direct modeling of x-ray diffraction pattern from skeletal muscle in rigor. Biophys J. 2002. 83:1082-97.

Huxley H.E., Stewart A., Sosa H., Irving T. 1994. X-ray diffraction measurements of the extensibility of actin and myosin filaments in contracting muscle. Biophys J. 67:2411-21.

Bordas J, Diakun GP, Diaz FG, Harries JE, Lewis RA, Lowy J, Mant GR, Martin-Fernandez ML, Towns-Andrews E. 1993. Two-dimensional time-resolved X-ray diffraction studies of live isometrically contracting frog sartorius muscle. J Muscle Res Cell Motil. 14(3):311-24.

Caremani M, Dantzig J, Goldman YE, Lombardi V, Linari M. 2008. Effect of inorganic phosphate on the force and number of myosin cross-bridges during the isometric contraction of permeabilized muscle fibers from rabbit psoas. Biophys J. 95(12):5798-808.